ARTICLE

Structural and molecular alterations in murine tissue due to far-field radiofrequency exposure

Aaron Paul T. Baliga*[1], Roy Francis R. Navea[2], Clarissa L. Velayo[1]

[1]Department of Physiology, College of Medicine, University of the Philippines - Manila, Philippines
[2]Department of Electronics and Communications Engineering, Gokongwei College of Engineering, De La Salle University, Manila, Philippines

ABSTRACT

Public concern over exposure to radiofrequency electromagnetic fields has prompted several studies to determine possible health outcomes. However, studies on low level far-field radiofrequency (RF) exposure remain inconclusive on whether it can alter biological systems. Our study's aim was to evaluate structural and molecular modifications such as apoptosis and gene expression in murine brain, liver and kidney tissues exposed to a far-field RF of 915 MHz at a whole-body specific absorption rate of 1.17 W/kg. Forty (40) Swiss male mice were equally and randomly divided into 2 groups: a control group and an RF-exposed group. Each were further equally subdivided (n=5 per subgroup) based on different time points: baseline or no exposure, 3-day exposure, 6-day-exposure and 9-day exposure subgroups. Biometric parameters such as body temperature, body weight, and organ weight were obtained. Tissue samples were collected and analyzed using light and electron microscopy, followed by qPCR assay for both the p53 and Hsp-70 genes. Statistical analysis was performed using ANOVA. There was evidence of both structural and molecular modification beginning Day 3 from continuous-wave far-field RF exposure. The study established multi-level alterations in the murine system due to far field RF exposure providing a glimpse of possible biological effects, and therefore, a need for further studies to translate such evidence in a larger biological perspective.

*Corresponding author
Email Address: atbaliga@up.edu.ph
Date received: October 19, 2023
Date revised: April 11, 2024
Date accepted: April 26, 2024
DOI: https://doi.org/10.54645/202417SupNFX-98

INTRODUCTION

Decades of research have focused on whether exposure to radiofrequency (RF) can cause significant biological effects. Modern devices such as cellphones and laptops rely on radiofrequency to become an integral part of modern society. It is considered non-ionizing radiation that operates under the vibrational rate of an alternating electric current or voltage, or a magnetic, electric, or electromagnetic field mechanical system with a different frequency range (Advisory Group for Non-Ionizing Radiation, 2012).

The escalating use of and worldwide engagement with non-ionizing radio-frequency devices may result in possible health outcomes (Vijayalaxmi 2014). This observation has been a cause for concern in both the social and scientific communities as there have been reported adverse health effects due to emissions from wireless technologies. In response, the World Health Organization (WHO) created the International Electromagnetic Field (EMF) Project that assesses scientific studies and pieces of evidence showing effects of the electromagnetic field on health (Repacholi 2001). The International Agency for Research on Cancer (IARC) under the World Health Organization also evaluates human cancer risks from electromagnetic field exposure and classifies

KEYWORDS

Far-field radiofrequency, hsp-70, p53, electron microscopy, specific absorption rate

electromagnetic field radiation as a possible carcinogen to humans (2B) (Cogliano et al. 2011). According to the report, exposure to RF radiation alters cellular metabolism, genetic integrity, oxidative balance, and biological function of exposed tissues. (Trosić 2011).

Several studies were conducted to assess possible epidemiological, in-vitro, and in-vivo outcomes with regard to the non-thermal effects of radio-frequency exposure in humans and animal subjects. Together, in-vivo and in vitro examination revealed that RF energy exposure turns into a biological stressor because the outcomes act as similar to stress reactions (Trosić 2011). Two possible mechanisms are involved in explaining biophysical and physiological alterations. Biophysically, a form of forced-vibration of free ions on the surface of a cell membrane and a moving charge interaction both cause apparent biological changes (Blank and Soo 2001; Panagopoulos et al. 2002; Panagopoulos et al. 2000). Concerning the physiological mechanism involved, several studies reported that RF waves emitted by mobile phones might cause many deleterious outcomes on cellular and molecular levels via DNA damage, oxidative stress, and an elevation of free radicals (Akdag et al. 2016; Chauhan et al. 2016; Dasdag and Akdag 2016; Deshmukh et al. 2013; Megha et al. 2015). In particular, in-vivo animal studies show that biological effects of reactive oxygen species' production leading to oxidative stress cause cascading cellular outcomes in radio-frequency exposure (Chauhan et al. 2016; Berköz et al. 2018; Yokus et al. 2008). Moreover, electromagnetic field exposure has also been seen to bring about apoptosis via oxidative stress and DNA damage (Alkis et al. 2019; Xing et al. 2016). Most effects though notable at a cellular level may show no difference at the organism level as seen in various studies where RF did not influence the mean body weight of study animals (Alimohammadi et al. 2018; Erpek et al. 2007; Krishna et al. 2019; Mai et al. 2020; Maskey et al. 2010; Sommer et al. 2004; Zhang et al. 2017).

Several studies that evaluated effects at a molecular level have documented that RF radiation-induced alterations in gene/ protein expression occur in various tissues (McNamee et al. 2009). The activation of p53 serves to upregulate pro-apoptosis genes. Simultaneously, heat shock protein-70 provided anti-apoptotic defense mechanisms both released in response to various stressors, while other studies show no apparent effects related to RF (Blank and Goodman 2009; Rérole et al. 2011). Overall, our study goal was to determine morphological and molecular alterations in murine tissues such as the brain, liver, and kidney exposed to continuous 900 Mhz GSM far-field radiofrequency with a specific absorption rate of 1.7 Watts/kilogram in 24 hours in freely moving test subjects. Effects were measured at specific post-exposure intervals with a maximum range of nine (9) consecutive days. Specifically, the study aimed to (1) compare body temperature, body weight, and organ weight between radiofrequency exposed animals and the control group, (2) compare apoptotic cell counts between radiofrequency-exposed animals and the control group, and (3) investigate p53 and HSP-70 gene expression in both animal groups.

MATERIALS AND METHODS

Experimental Animals and Treatment Groups. Forty (40) 6-week old Swiss albino (ICR) male mice weighing 30-34 grams were purchased from the Veterinary Research Department, Research Institute for Tropical Medicine, Philippines. All animal procedures and experiments were done in accordance with the University of the Philippines-Manila, Research Ethics Board guidelines, under a protocol approved by the National Institute of Health-Institutional Animal Care and Use Committee (protocol number 2019-027). The animals were placed in polypropylene cages, measuring 25 cm x 7 cm x 7 cm with ventilation holes. Commercial wood chip bedding was replaced twice weekly. The mice were kept in a controlled setting (20ºC- 24ºC temperature, 62%-70% humidity) with a 12h light cycle (07:00 H–19:00 H) at all times and were given access to Mazuri® rat and mouse pellets (#5663, PMI Nutrition International, LLC, MN, USA) and distilled water ad libitum. The mice were acclimated for five days prior to testing, and then were randomly allocated to treatment groups.

Treatment groups. Mice were randomly assigned into two groups: a Control (C) group (n=20), which was subjected to a sham setup, and a Radiofrequency (RF) group (n=20), which was exposed to a radiofrequency setup (Figure 1). Mice in both groups were further subdivided as follows: (1) Baseline with no RF exposure (n=5), (2) 3-days RF exposure (n=5), (3) 6-days RF exposure (n=5), and (4) 9-days RF exposure (n=5). Body temperatures and body weights were routinely recorded each day. The body temperature of the mouse was obtained using an infrared thermometer without anesthetics.

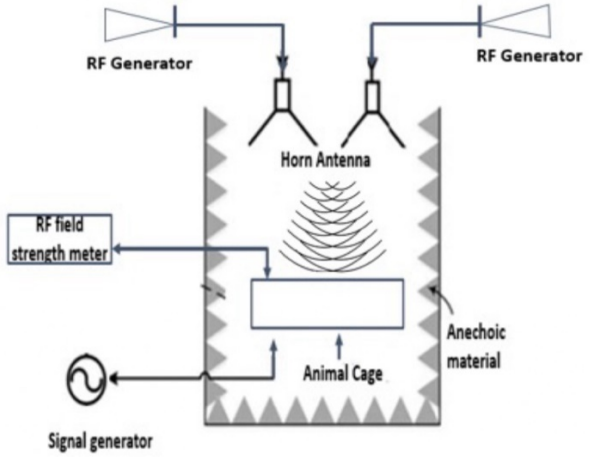

Figure 1: Radiofrequency Radiation (RFR) exposure setup.

Radio-frequency exposure system and condition. The RF group was exposed to a 24-hour continuous wave system with a specific radiofrequency of 915 Megahertz (Mhz). The radiofrequency exposure system comprised of a radiofrequency generator (Lab-Volt-9505-05, Festo Didactic Inc, Germany) with two (2) horn stationary antennae (Lab-Volt-D-79360, Festo Didactic Inc, Germany), which was customized to produce an electromotive force equal to that discharged by global systems for mobile communications (GSM) mobile phones – 915 megahertz (MHz) and monitored using a radio-frequency Spectrum Analyzer (PSA2702 2.7 GHz RF Spectrum Analyzer, Saelig Company Inc, NY, USA) to remain within a frequency range of 1 to 2700 Mhz and bandwidth of 30 MHz to 1.8 Gigahetrz (GHz) (figure 1). The two horn antennae were placed above the exposure site at a height of 70 cm from the ground with an area measurement of 71.25 cm x 60 cm on both sides of the chamber at the same frequency to distribute the electric field evenly. Furthermore, an anechoic material (foam) that acted as a reflective wall was used in the RF-exposed group, reflecting the chamber's electric field inside the testing area. The maximum electric field emitted in the RF radiation system was measured using three axis high-frequency RF field strength meters (Tenmars 3 axis high frequency RF field strength meter TM-195, Test Meter Group Ltd, UK), all with a measuring range of 50 MHz-3.5 GHz. In the study, the electric field was characterized by measuring the electromagnetic wave in free space (ERMS) for 1 minute at the positions of the head, body, and tail of the mice during the exposure, and this was repeated 3 times.

Three (3) days before actual RF field exposure, all animals were weighed and body temperatures were obtained using an animal infrared thermometer (ZERO ONE DT-8866, China) at 24-hour intervals. The RF groups were acclimated within the RF setup before the onset of exposure periods. On the day of exposure, the RF radiation system was energized and allowed to operate for 15 minutes before the onset of animal exposure. Actual RF exposure entailed continuous maintenance of the animal cage within the active set-up for 24 hours lasting between 3 to 9 days. The mice were placed not more than 40 cm from the horn antenna.

Estimation of Whole-Body Specific Absorption Rate. The whole-body specific absorption rate (SAR) was the dosimetric parameter obtained for this particular biological system. The SAR or the rate of energy absorbed by tissue was calculated using both conductivity and dielectric constants. The whole-body SAR estimation used based on the study of Esmekaya et al. in 2011 adopted an average conductivity value of $\boldsymbol{\sigma}$ =0.87 Siemens/meter, used an estimated density $\boldsymbol{\rho}$ of 1050 kg/m^3, and used $\boldsymbol{E}$ the root mean square value of the electrical field which was approximately 37.5 Volt/meters. Also, $\boldsymbol{\sigma}$ was the mean electrical conductivity of the tissue (S/m) and $\boldsymbol{\rho}$ the mass density of the tissue (kg/m^3) which were 0.87 S/m and 1050 kg/m3, respectively (Repacholi 1998). In the study, the electric field (ERMS) was detected by measuring the electrical fields for 1 minute at the positions of the head, body, and tail of the mice during the exposure, which was repeated 3 times. The electric field was defined as the average of measurements at the three parts of the body. The average electric field (RMS) in the study is approximately 37.5 volts/meter. The SAR calculated in Watts per kilogram was the following:

$$SAR = \frac{\boldsymbol{\sigma}\, \boldsymbol{E_i^2}}{\boldsymbol{\rho}}$$

$$SAR = \frac{0.87 \frac{S}{m} \left(37.5 \frac{V}{m}\right)2}{1050 \frac{kg}{m3}} = 1.17\ \mathrm{W/kg}$$

Tissue sampling. Immediately following the control and exposure groups' treatments, the mice were sacrificed by cervical dislocation. Organs subsequently harvested included the brain, liver, and kidneys, and these were placed in pre-chilled Petri dishes with 5 ml RNA SaveTM preservative solution (Biological Industries (BI), Kibbutz Beit Haemek 25115, Israel) and decontaminated using RNaseZapTM (Sigma-Aldrich, Merck KGaA, Darmstadt, Germany) to prevent autolysis. Organs were weighed and then carefully transferred into 5 ml RNase free conical tubes and stored in -20°C overnight.

Light and Electron Microscopy. One organ sample per treatment group was randomly selected for light microscopy analysis. Organs were blotted on a sterile pad to remove RNA preservative solution and fixed in 10% formaldehyde for 72 hours. This was followed by routine paraffin waxing, and sequential cutting into 5-micrometer slices (Leica RM2125 Microtome, Florida, USA). Tissues were stained utilizing Hematoxylin and Eosin (H & E), and representative samples were photographed. Each tissue was analyzed by counting the apoptotic cells in 5 different random areas from each of the sample slides. Microscopic examination (Olympus BX41, Tokyo, Japan) for apoptotic cell bodies was performed at ten (10) x magnification and performed by a pathologist blinded to the experiment.

In addition, 4 brain samples per treatment were blotted and at the cerebral region cut transversely into 3-millimeter slices for scanning electron microscopy. Cut tissues were thrice washed with a phosphate buffer with a pH of 7.4. Sample tissues were initially fixed using 2.5% glutaraldehyde for 24 hours, followed by fixing for two (2) hours using 1% OsO4 (osmium tetroxide), then washed three times for fifteen (15) minutes each using a phosphate buffer with a pH of 7.4. Samples then underwent a series of dehydration cycles with ethanol at varying concentrations: 35% ethanol for fifteen (15) minutes, 50% ethanol for fifteen (15) minutes, 75% ethanol for fifteen (15) minutes, 95% ethanol for fifteen (15) minutes twice, and absolute ethanol for twenty (20) minutes thrice. Then, the dehydrated tissues were immersed for ten (10) minutes twice using 1-2 ml Hexamethyldisilazane (HMDS). Traces of HMDS were removed, and sample tissues were placed in a vial and left overnight in a desiccator at room temperature. The sample was gold-sputtered using a fine coater (JEOLTM JFC-1200 fine coater, USA) with about 5–10 nanometers of gold before viewing. Lastly, representative samples were then mounted onto a scanning electron microscope (SEM) stub with an adhesive carbon strip for viewing (Phenom XL desktop Scanning Electron Microscope, Eindhoven, The Netherlands).

RNA isolation and Quantitative Polymerase Chain Reaction (qPCR). To examine the molecular effects of RF exposure, qPCR was performed for two selected genes, p53 and HSP-70. Total RNA was extracted from the mice organs (brain, liver, and kidneys) per treatment (n=3) using a nucleic acid extraction kit (GF-1 Nucleic acid extraction Vivantis Technologies, Malaysia) following the manufacturer's protocol (see Appendix E). Each RNA concentration was assessed using a NanoDrop spectrophotometer (DeNovix DS-11 Spectrophotometer/ Fluorometers and NanoDrop™, USA). An A260/A280 ratio of 1.8-2.2 was indicative of highly purified RNA. RNA integrity was tested using agarose gel electrophoresis, stained with ethidium bromide in each lane using a horizontal electrophoresis system (MS 3AP power supply, USA) under 100 volts for 1 hour. Visualization of bands on the gel was performed using a Bio-Rad ChemiDoc™ MP Gel Imaging System (USA) and assessed for 18S rRNA and 28s rRNA bands to verify RNA integrity. Samples were stored in an -80°C freezer.

The p53 and Hsp-70 qPCR assay was performed using ViPRimePLUS One Step Taq RT-qPCR Green Master Mix I (Vivantis Technologies, Malaysia) under the following conditions: A 30-nanogram (ng) RNA sample was placed into a 20 µL reaction volume containing 0.2 µM of each primer, 10 µL of SYBR green I RT-PCR one-step master mix (Vivantis Technologies, Malaysia), and 0.2 µL of reverse transcriptase. The protocol included reverse transcription at 50°C for 30 minutes, denaturation at 95°C for 15 minutes, and 40 cycles of denaturation at 94°C for 15 seconds, annealing of 57°C for 30 seconds, and extension at 72°C for 30 seconds. Real-time detection of emission intensity of SYBR Green bound to cDNA was analyzed using Bio-Rad *CFX96* Touch™ Real-Time PCR Detection Systems (USA). Beta-actin mRNA was utilized as a reference gene to calculate the relative expression of the target genes. All samples were run in triplicate. The primer sequences in this study are listed in Supplementary Table 1.

Statistical Analysis. STATA/SE software 14.0 (StataCorp Inc., Lakeway Drive, Texas, USA) was used to perform the statistical analyses. All data were presented as the average (mean) ± SD of each group. Statistical analyses were performed using a two-way Analysis of Variance (ANOVA), and Tukey's post hoc test was used to verify the statistical difference between groups. Differences with $p < 0.05$ were considered statistically significant. For qPCR evaluation, Ct values were normalized against the reference gene, beta-actin, using the following formula: ΔCt = Ct gene of interest - Ct reference gene.

RESULTS

Biometric Parameters

Effect on Body Temperature. The mean body temperature was statistically different between the experimental group and the control group (F=44.01; p<0.0001) (Table 1). Mice in the RF-exposed group showed a higher mean body temperature from day 3 to day 9. Furthermore, Tukey's pairwise comparison showed that the mean body temperature of the RF-exposed group in each time point such as in the 3-day exposure (t=5.44; p<0.001), 6-day exposure (t=10.55; p<0.001), and 9-day exposure (t=11.88; p<0.001) were statistically different from the baseline with an increase of more than 1°C. The mean body temperature of animals exposed to RF for 3 days, 6 days, and 9 days is higher compared to baseline. The mean body temperatures of mice (RF exposed) belonging to the 6-day exposure, and the 9-day exposure were statistically different from those with 3-day exposures (Table 1).

Table 1: Mean body temperature of control and RF (experimental) exposed mice in each time points.

Time points	Control (°C)	Experimental (°C)
Baseline	35.36 ± 0.14	35.17 ± 0.13
3-Day Exposure	35.33 ± 0.17	35.99 ± 0.25*
6-Day Exposure	35.37 ± 0.12	36.7 ± 0.11*
9-Day Exposure	35.23 ± 0.16	37.04 ± 0.18*

Note: The values are means ± SD; n = 20 in each group. p < 0.05 is significant(*)

Effect of on Body Weight. Table 2 showed that there were no significant changes observed in the mean body weights of study animals in the RF and control groups (F=1.60; p=0.2145) and therefore no significant differences between them.

Table 2: Mean body weight of control and RF (experimental) exposed mice in each time point.

Timepoints	Body temperature	
	Control (g)	Experimental (g)
Baseline	34.77 ± 1.68	34.08 ± 1.84
3-Day Exposure	38.06 ± 2.64	37.19 ± 2.77
6-Day Exposure	40.99 ± 3.22	40.06 ± 2.84
9-Day Exposure	43.52 ± 2.05	42.05 ± 3.23

Note: The values are means ± SD; n = 20 in each group. p < 0.05 is significant

Effect of Organ Weight. In terms of the murine brain weight (F=0.16; p=0.6909), there was no statistically significant change noted secondary to the length of exposure or treatment conditions (Table 3). While controlling for the effects of days of treatment, there was no sufficient evidence to say that the mean kidney weight differed between treatment groups (F=2.62; p=0.1148) (Table 4).

Table 3: Mean brain weight of control and RF (experimental) exposed mice in each time point.

Timepoints	Brain weight	
	Control (g)	Experimental (g)
Baseline	0.45 ± 0.03	0.42 ± 0.04
3-Day Exposure	0.52 ± 0.05	0.50 ± 0.02
6-Day Exposure	0.48 ± 0.03	0.52 ± 0.04
9-Day Exposure	0.49 ± 0.07	0.52 ± 0.04

Note: The values are means ± SD; n = 20 in each group. p < 0.05 is significant

Table 4: Mean kidney weight of control and RF (experimental) exposed mice in each time point.

Time points	Kidney weight	
	Control (g)	Experimental (g)
Baseline	0.59 ± 0.05	0.56 ± 0.07
3-Day Exposure	0.53 ± 0.09	0.63 ± 0.06
6-Day Exposure	0.53 ± 0.09	0.54 ± 0.08
9-Day Exposure	0.58 ± 0.07	0.66 ± 0.07

Note: The values are means ± SD; n = 20 in each group. p < 0.05 is significant

There was a statistical difference in mean liver weight among RF groups as compared to the control group (F=4.16; p=0.0490). Overall, liver samples in the RF groups were slightly heavier than their counterpart control samples (Table 5).

Table 5: Mean liver weight of control and RF (experimental) exposed mice in each time point.

Time points	Liver weight	
	Control (g)	Experimental (g)
Baseline	1.41 ± 0.14	1.54 ± 0.34
3-Day Exposure	1.63 ± 0.36	1.72 ± 0.33
6-Day Exposure	1.27 ± 0.11	1.38 ± 0.14
9-Day Exposure	1.74 ± 0.11	2.09 ± 0.37

Note: The values are means ± SD; n = 20 in each group. p < 0.05 is significant

Histologic and Morphometric Assessment of Murine tissues

The results showed increasing apoptotic cell counts over the whole time course of observation (F[3, 104] = 120.88, p < 0.01) in all tissues examined. Although there was no significant difference from baseline to Day 3 (t = 1.30, p = 0.43) of observation, it was noted that apoptotic changes were significantly higher from Day 3 to Day 6 (t = 3.14, p = 0.01), and to Day 9 (t = 7.50, p<0.01). Tukey's comparison procedure also showed that RF treatments had significantly higher apoptotic cell counts compared to the control group (F[1, 104] = 64.67, p<0.01). Furthermore, it was noted that murine brain tissue appeared to have significantly higher apoptotic changes compared to those of the kidneys and the liver (F[2, 104] = 15.70, p<0.01) (Table 6).

Table 6: Mean apoptotic cell counts in different murine tissues at each time points.

	Apoptotic cell count	
	Control	Experimental
Brain		
Baseline	0 ± 0	0 ± 0
3-Day Exposure	0 ± 0	1.60 ± 0.89*
6-Day Exposure	1.20 ± 0.45	5 ± 0*
9-Day Exposure	1.80 ± 1.30	13.20 ± 1.92*
Kidney		
Baseline	0 ± 0	0 ± 0
3-Day Exposure	0 ± 0	1.20 ± 0.45*
6-Day Exposure	0.80 ± 0.45	3 ± 0.71*
9-Day Exposure	1.80 ± 0.84	5.40 ± 0.55*
Liver		
Baseline	0 ± 0	0 ± 0
3-Day Exposure	0 ± 0	1 ± 0
6-Day Exposure	0.40 ± 0.55	1.20 ± 0.45*
9-Day Exposure	1.60 ± 0.55	3.40 ± 4.28*

Note: The values are means ± SD; p < 0.05 is significant(*)

Light microscopy showed that murine tissues of RF-exposed mice exhibited characteristic shrinkage formation of the cell and fragmentation into membrane-bound apoptotic bodies both indicating the ongoing development of apoptosis during the different periods of exposure. Apoptotic bodies are small, membrane-bound vesicles that are formed during the process of apoptosis, which is a controlled and programmed form of cell death. The formation of apoptotic bodies is one of the key morphological features of apoptosis. Some characteristics of apoptotic bodies: size and structure (apoptotic bodies are typically small, membrane-bound vesicles ranging from 1 to 5 micrometers in diameter), origin, cellular contents, membrane integrity and recognition, and clearance (Figure 2).

Figure 3 shows SEM micrographs of murine brain tissue in the RF-exposed group at baseline (Figure 3A) and compared to micrographs of the cerebrum with different time levels of exposure to continuous radiofrequency radiation (Figures 3B-D).

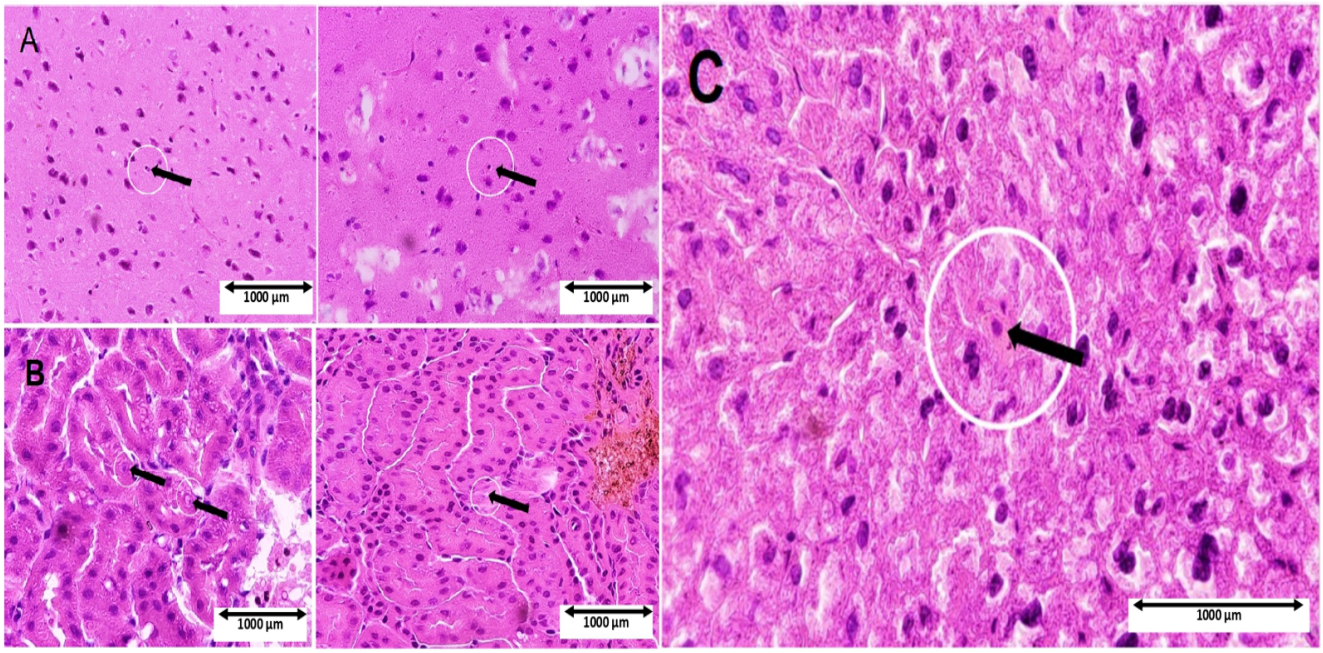

Figure 2: Photograph of murine tissue (stained with hematoxylin and eosin) such as (**A**) brain, (**B**) kidney, and (**C**) liver are showing apoptotic cell bodies (pointed by black arrow) following exposure to far-field radiofrequency. A light microscopy examination for apoptotic cell bodies was done using ten high power fields in 5 different areas of tissue slide for the RF-exposed group.

As compared to normal morphology at baseline, RF exposed tissue revealed several characteristic structural deformations like swelling, kinking, twisting, and looping. In the third day of exposure (Figure 3B), several circular surface "bleb like" structures (30 µm) were observed. The progressive effects of RF exposure were seen in the sixth (Figure 3C) and ninth days (Figure 3D) as elongated dense granular-irregular shaped surface lesions with an amorphous fibrous like appearance.

Microarray analysis of p53 and HSP-70 genes

Figure 4 illustrates gene expression patterns of p53 and HSP-70. For p53 (Figure 4A), there was a significant difference in expression levels in the brain of the RF-exposed group compared to the control group (F=7.65; p=0.0123), the expression level of p53 and HSP-70 of the RF exposed group was higher than the control group. Also, Tukey's comparison test revealed that gene expression of p53 in murine tissues was significantly higher on day-9 compared to other time points. Similarly, HSP-70 expression (Figure 4B) of the brain in the RF-exposed group was significantly different compared to the control group (F=15.02; p=0.0010). In terms of exposure time, the Tukey's comparison test showed that the RF group gene expression of p53 and HSP-70 on day 6 (t=3.64; p=0.009) and on day 9 (t=4.40; p=0.002) were significantly higher than baseline levels. In addition, liver and kidney showed an increase expression level of p53 and HSP-70 in RF exposed mice compared to the control group.

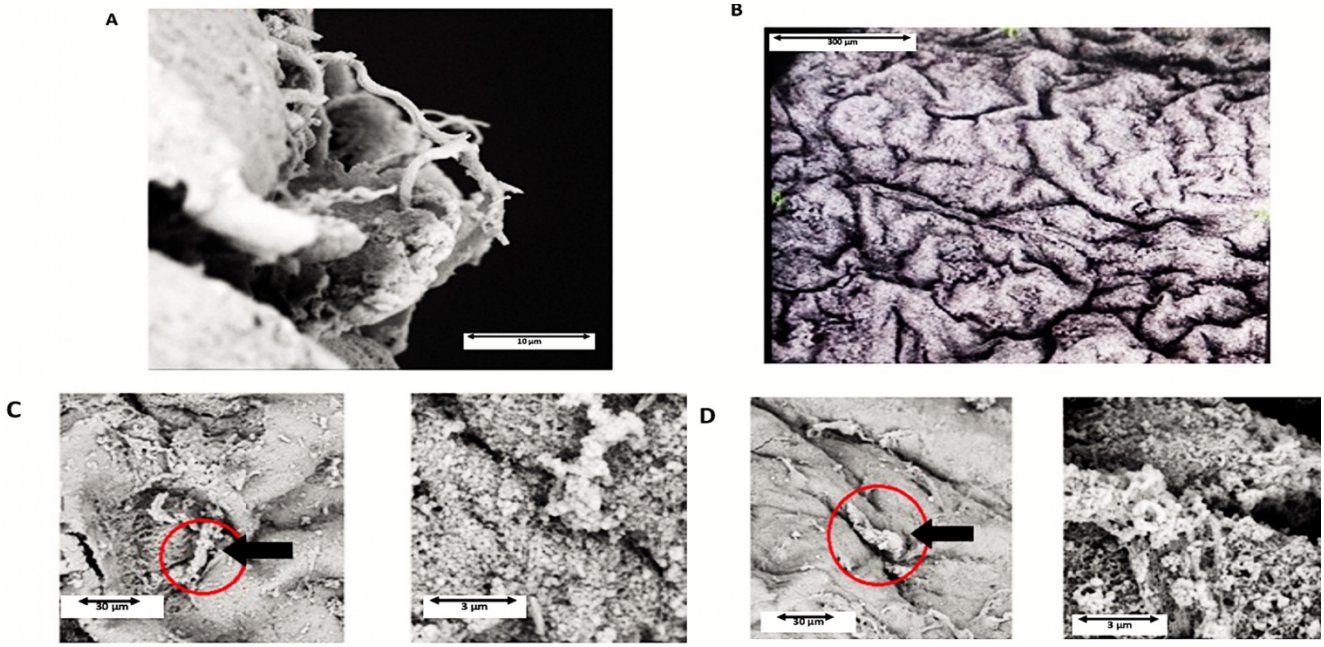

Figure 3: Electron microscopy analysis. Scanning electron microscope images of the surface morphology of the murine cerebrum exposed to continuous far-field radiofrequency at different time points: (**A**) baseline; (**B**) 3-day-exposure with "bleb like" structure (30 µm) observed (encircled in red with a black arrow); (**C**) 6- day exposure and (**D**) 9- day exposure samples with elongated dense granular-irregular shaped surface lesions with an amorphous fibrous like appearance (encircled in red with a black arrow).

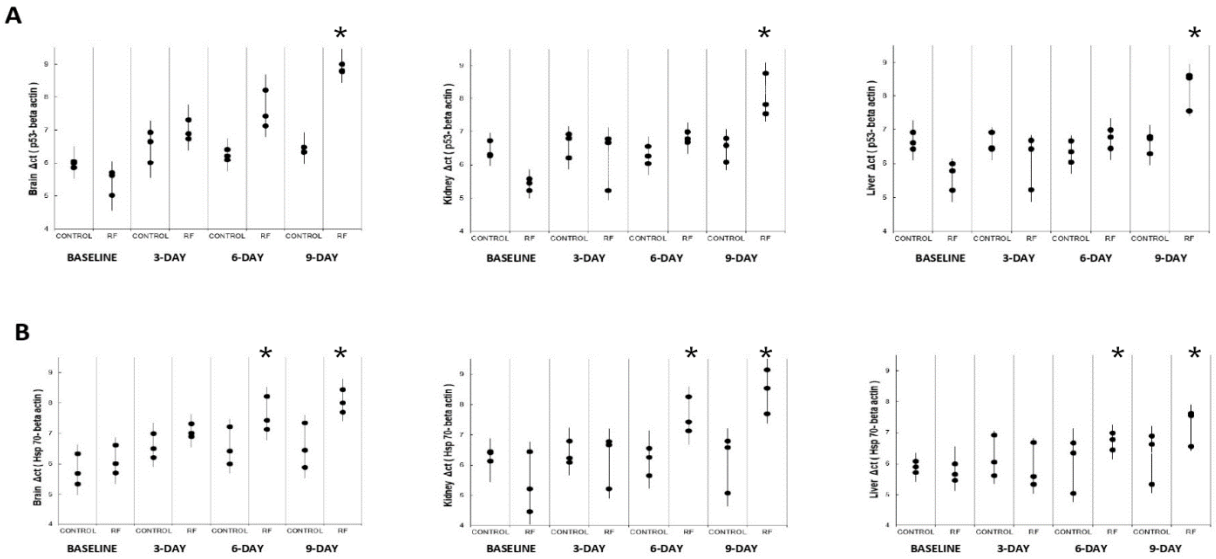

Figure 4: Gene expression patterns of p53 (A) and HSP-70 (B).

DISCUSSION

In this present study, mice exposed to a continuous 900-Mhz far-field radiofrequency with SAR equivalent to 1.7 W/kg displayed higher body temperatures as compared to baseline control groups. Compared to existing studies (Gordon et al. 1986; Wyde et al. 2018; Kim et al. 2020), the observed elevations in temperature of our experimental animals were all within the limits of safety standards. Based on existing guidelines, an elevation of temperature by 1°C in SAR ranging from 1 W/kg to 4 W/kg from exposure to high field, low-intensity RF maintains a normal physiological state in humans as there are no thermoregulatory changes brought about by this temperature elevation (Repacholi 1998; Trošić et al. 2012). Likewise, temperature changes within the range of 1°C are considered as only thermal noise (Vornoli et al. 2019). The prevailing view is that RF energy absorption may cause induction of an endogenous heat source, which in turn is added to the mouse's metabolic heat production, causing elevation of body temperature. However, our findings using a murine model suggest that RF exposure within the allowable safety limit can still initiate a biological system's thermal response. Since the animal was exposed to a continuous wave of far-field radiofrequency, progressive change in temperature may suggest adaptation rather than a thermoregulatory malfunction; however, an explanation of thermal adaptation is not within the scope of the study. Therefore, while there were temperature increases caused by RF exposure, they were not clinically relevant as the temperatures were within the normal physiological range regardless of statistical significance (Repacholi 1998).

Alternatively, biophysical mechanisms may also explain how radiofrequency exposure can elevate body temperature. One basic principle governing RF's thermal effect is the law of conversion of energy, wherein absorbed RF energy can be converted via the increased kinetic energy of absorbing molecules. This energy produces heating in tissue because animals, such as the mouse, are poor electromagnetic irradiators due to body composition thus, most of the RF energy is converted into heat. Specifically, a mechanism for tissue heating is explained via the field-induced rotation of polar molecules, primarily due to the rotation of water molecules present in the biological system, in this case, the mouse's body composition. This mechanism occurs through Brownian motion which helps water molecules become rearranged and broken in a normal state, but radio frequencies, mainly through an electric field, restructure the molecules. Underneath this condition, polar water rotates to conserve orientation within a time-varying electric field. The mechanism is fast-breaking and reconfiguration of water molecules brought by mechanical interactions resulting in frictional forces lead to heat (Repacholi 1998; Stuchly 1979).

On the other hand, in this study the 900 MHz far-field radiofrequency exposure did not reveal any statistically significant differences in the mean body weight and organ weight between RF exposed and baseline control animals. Hence, continuous exposure to a low-frequency electromagnetic field does not appear to have affected these biometric parameters. The findings are in line with earlier results that RF exposure does not influence the mean body or organ weight of animals (Alimohammadi et al. 2018; Erpek et al. 2007; Krishna et al. 2019; Mai et al. 2020; Maskey et al. 2010; Sommer et al. 2004; Zhang et al. 2017). Nonetheless, both animal groups' weights increased over time primarily because of unlimited access to food and water (Erpek et al. 2007; Zhang et al. 2017). One possible explanation of how radiofrequency can affect a mouse's body weight is if discomfort or a disturbance of the circadian rhythm is present leading to decreased preferential food and water intake. However, there were no observable changes in the RF-exposed group's feeding habits compared to that of the baseline control group as each consumed food ad libitum.

In addition, morphological examination showed increased apoptotic counts after continuous exposure to a far-field radiofrequency of 915 MHz for nine days. In general, assessment using light and electron microscopic examination of the tissues such as the brain, liver, and kidneys from the RF-exposed group revealed a remarkable change in their apoptotic counts while there was intact structural integrity noted in the baseline control group. Significantly, the latter observable degree of histological alteration also increased over time in all tissues with RF-exposure. In summary, the evidence supports the change in apoptotic counts observed in tissues from the RF-exposed group, as well as indicates that the degree of histological alteration increases over time. This provides a basis

for inferring a relationship between the duration of RF exposure, the progression of apoptotic events and the histological changes in examined tissues.

Further data analysis revealed a marked increase in the number of apoptotic counts in the brain more than the liver and the kidney. Moreover, electron microscopy of mice cerebral cortices revealed changes in surface morphology. These were characterized by various types of deformation like swelling, several circular surface "blebs," and lesions that were elongated dense granular irregularly-shaped structures with an amorphous fibrous like appearance. These structural deformities were also observed in neural tissue transplants in a mouse model for Alzheimer's disease; however, comparison of our findings is limited as there are no available studies at present that have investigated the surface morphology of tissues exposed to radio frequencies. Brain tissues are considered to be electromagnetic field sensitive because of their ability to absorb high intensity electric and magnetic fields. Resonance signals detected by the brain may synchronize with its extremely low-frequency activity and cause neuronal cell apoptosis, altering the physiology of nerve myelin and ion channels. (Carrubba et al. 2009).

By far, the dominant mechanism by which radiofrequency energy can cause apoptosis is via the induction of oxidative stress such as with reactive oxygen species (ROS) or free radicals by means of a non-thermal effect. Harmful biological effects of ROS in the cellular milieu can include DNA level and protein level damages, the release of oxidative markers, and cellular apoptosis (Liu et al. 2013; Li et al. 2003). Despite being non-ionizing, RF energy can elicit considerable stimulation of free radical processes and increase the production of ROS in the biological system. There are several known physiologic and biochemical pathways that are associated with ROS, which includes lipid peroxidation or increased concentrations of malondialdehyde, protein peroxidation, increased concentrations of nitric oxide (NO), and changes in the activity of antioxidant enzymes. Earlier research proposed that RF exposure may disturb the biological system by elevating the ROS level and leading to oxidative stress (Singh et al. 2018; Zmyślony et al. 2004). Furthermore, this exposure alters the redox milieu by influencing biochemical signals within physiological limits and generating adaptive responses to stress.

Lastly, molecular analyses showed a significant increase in p53 and HSP-70 expression in the brain after continuous exposure to a far-field radiofrequency of 915 MHz for nine days with SAR of 1.7 W/kg. Like the brain, the liver and kidney showed statistically higher expression of p53 and HSP- 70 with continuous exposure, especially on the ninth day although not statistically significant. The study's result demonstrated the possible interaction of RF energy at a molecular level causing appropriate physiological responses in gene expression.

The theorized possible mechanism is a two-stage process that seemingly creates cascading cellular machinery leading to DNA bond breakage and altered gene expression. The dominant mechanism likely involves increased production of reactive oxygen species caused by deep penetration of RF in living tissue. ROS are generally small metabolically active short-lived molecules connected to oxidative stress. The preliminary stage of the ROS production in RF is regulated by the NADPH oxidase enzyme found in the plasma membrane. Membrane-associated enzymes such as NADH oxidase catalyze the one-electron reduction of oxygen into a superoxide radical using NADH as a donor of an electron, thus producing potent ROS (Kivrak et al. 2017; Yakymenko et al. 2015). Alternatively, some studies discovered a potential physiological role of ROS in regulating and promoting Ca2+ signaling by elevating intracellular Ca^{2+} concentration. Ca^{2+} is then released in the cytosol via the endoplasmic reticulum (ER), extracellular space, or mitochondria in response to oxidase-influence on Ca^{2+} pumps, channels, and transporters. Other studies have revealed such a related interplay between Ca^{2+} signaling and ROS (Görlach et al. 2015). This aligns closely with the observed effects of the study, wherein exposure to a continuous wave 900 MHz GSM far-field signal led to more apoptosis and altered gene expression, particularly of p53 and HSP-70. The findings of the molecular analysis, which showed increased p53 and HSP-70 expression in the brain, liver, and kidney after continuous exposure to radiofrequency (RF) radiation, are related to the theorized mechanism involving the production of reactive oxygen species (ROS) and its impact on DNA damage and gene expression. Several studies have demonstrated that RF radiation can significantly increase ROS production, leading to oxidative damage to cellular components, including DNA. The increased expression of p53 and HSP-70 in the brain, liver, and kidney following RF exposure suggests a potential link to the generation of ROS and the resulting physiological responses in gene expression. The production of ROS in RF exposure is regulated by enzymes such as NADPH oxidase, which catalyze the one-electron reduction of oxygen into superoxide radicals, contributing to the cascade of cellular machinery leading to DNA damage and altered gene expression. Additionally, ionizing radiation, including RF, can directly induce DNA breaks and generate ROS, leading to DNA damage and altered gene expression. Therefore, the increased expression of p53 and HSP-70 in the brain, liver, and kidney following RF exposure may be attributed to the two-stage process involving ROS production and its impact on DNA damage and gene expression.

Interestingly, control groups exhibited expression patterns of p53 and HSP-70 in murine tissue. It is essential to highlight that these animals were not entirely free from RF-exposure. Although the latter did not receive a continuous RF-exposure wave, they could still have been exposed to RF stray signals and frequencies from different surrounding locations such as schools, offices, and warehouse factories in the vicinity. During acclimatization, both animal groups were kept in the same room and may have received RF stray signals. These low-level intensity radio frequencies may have affected the cellular tissue of controls, as well as caused ROS production leading to the expression of targeted genes at a lesser degree.

In summary, low-level intensity continuous far-field region exposure revealed patterns of change within a murine model. Based on the experimental procedures, exposure to a continuous-wave 900 Mhz GSM far-field signal with a specific absorption rate of 1.17 W/kg caused cellular and molecular level effects. The physiological and biophysical observed alterations were temperature changes, increases in apoptotic cell count, and molecular expression of targeted genes such as p53 and HSP-70. All these strongly indicated the capacity of an electromagnetic field to induce changes in a complex biological milieu. However, the results may indicate physiological rather than pathological consequences.

CONCLUSION

In conclusion, the results strongly support the notion that electromagnetic fields, particularly the 900 MHz GSM signal studied, have the capacity to induce complex changes in a biological milieu. The observed effects at both physiological and biophysical levels, including temperature changes, increased apoptosis, and altered gene expression, underscore the sensitivity of living organisms to low-level EMF exposure. However, it is crucial to note that the results may point towards physiological rather than pathological consequences. While the observed changes indicate a significant biological response,

further research is needed to ascertain the long-term implications and whether these alterations lead to adverse health effects. The findings contribute to the ongoing discussion on the potential impact of electromagnetic fields on living organisms and highlight the need for continued investigation into the mechanisms underlying these observed effects.

FUNDING

APT Baliga is a Philippine Department of Science and Technology (DOST) Scholar.

ACKNOWLEDGMENT

The author would like to thank collaborators from De La Salle University, Laguna Campus, Philippines through the endorsement of Gil N. Santos.

CONFLICT OF INTEREST

The authors declare that the research was conducted in the absence of any commercial or financial relationships that could be construed as a potential conflict of interest.

CONTRIBUTIONS OF INDIVIDUAL AUTHORS

APTB is the sole first author and corresponding author. Conceptualization, Methodology, Conduction, Analysis and Original Draft Writing of the Research were contributed by APTB. Conceptualization, Methodology and Resources for this research were contributed by RFRN. Conceptualization, Methodology, Analysis, Manuscript Writing Review, Editing, and overall Supervision of the research were contributed by CLV.

REFERENCES

Akdag MZ, Dasdag S, Canturk F, Karabulut D, Caner Y, Adalier N. Does prolonged radiofrequency radiation emitted from Wi-Fi devices induce DNA damage in various tissues of rats? J Chem Neuroanat 2016; 75(Pt B):116-22.

Alimohammadi I, Ashtarinezhad A, Asl BM, Masruri B, Moghadasi N. The effects of radiofrequency radiation on mice fetus weight, length and tissues. Data Brief 2018; 30;19:2189-2194.

Alkis ME, Bilgin HM, Akpolat V, Dasdag S, Yegin K, Yavas MC, Akdag MZ. Effect of 900-, 1800-, and 2100-MHz radiofrequency radiation on DNA and oxidative stress in brain. Electromagn Biol Med 2019; 38(1):32-47.

Berköz, M., Arslan, B, Yıldırım M, Aras N, Yalın S, Çömelekoğlu Ü. 1800 MHz radio-frequency electromagnetic radiation induces oxidative stress in rat liver, kidney and brain tissues. EJM 2018; 23(2): 71-78.

Blank M, Goodman R. Electromagnetic fields stress living cells. Pathophysiology 2009; 16(2-3):71-8.

Blank M, Soo L. Electromagnetic acceleration of electron transfer reactions. J Cell Biochem 2001; 81(2):278-83.

Chauhan P, Verma HN, Sisodia R, Kesari KK. Microwave radiation (2.45 GHz)-induced oxidative stress: Whole-body exposure effect on histopathology of Wistar rats. Electromagn Biol Med. 2017; 36(1):20-30.

Cogliano VJ, Baan R, Straif K, Grosse Y, Lauby-Secretan B, El Ghissassi F, Bouvard V, Benbrahim-Tallaa L, Guha N, Freeman C, Galichet L, Wild CP. Preventable exposures associated with human cancers. J Natl Cancer Inst 2011; 103(24):1827-39.

Dasdag S, Akdag MZ. The link between radiofrequencies emitted from wireless technologies and oxidative stress. J Chem Neuroanat 2016; 75(Pt B):85-93.

Deshmukh PS, Megha K, Banerjee BD, Ahmed RS, Chandna S, Abegaonkar MP, Tripathi AK. Detection of low level microwave radiation induced deoxyribonucleic acid damage vis-à-vis genotoxicity in brain of Fischer rats. Toxicol Int 2013; 20(1):19-24.

Esmekaya MA, Ozer C, Seyhan N. 900 MHz pulse-modulated radiofrequency radiation induces oxidative stress on heart, lung, testis and liver tissues. Gen Physiol Biophys 2011; 30(1):84-9.

Erpek S, Bilgin M, Doger FK. The effect of electromagnetic field (50 HZ, 6mT) on rat liver and kidney. *Meandros Medical and Dental Journal* 2007; 8(1): 5-11.

Gordon CJ, Long MD, Feilner KS, Stead AG. Body temperature in the mouse, hamster, and rat exposed to radiofrequency radiation: An interspecies comparison. J of Thermal Biology 1986; 11 (1): 59-65.

Görlach A, Bertram K, Hudecova S, Krizanova O. Calcium and ROS: A mutual interplay. Redox Biol 2015; 6: 260-271.

Kim HS, Lee YH, Choi HD, Lee AK, Jeon SB, Pack JK, Kim N, Ahn YH. Effect of exposure to a radiofrequency electromagnetic field on body temperature in anesthetized and non-anesthetized rats. Bioelectromagnetics 2020; 41(2):104-112.

Kivrak EG, Altunkaynak BZ, Alkan I, Yurt KK, Kocaman A, Onger ME. Effects of 900-MHz radiation on the hippocampus and cerebellum of adult rats and attenuation of such effects by folic acid and *Boswellia sacra*. J Microsc Ultrastruct 2017; 5(4):216-224.

Krishna Kishore G, Venkateshu K, Sridevi N. Effect of 1800-2100 MHz electromagnetic radiation on learning-memory and hippocampal morphology in swiss albino mice. J Clin Diagn Res 2019; 13(2):14-17.

Li N, Ragheb K, Lawler G, Sturgis J, Rajwa B, Melendez JA, Robinson JP. Mitochondrial complex I inhibitor rotenone induces apoptosis through enhancing mitochondrial reactive oxygen species production. J Biol Chem 2003; 278(10): 8516-25.

Liu C, Duan W, Xu S, Chen C, He M, Zhang L, Yu Z, Zhou Z. Exposure to 1800 MHz radiofrequency electromagnetic radiation induces oxidative DNA base damage in a mouse spermatocyte-derived cell line. Toxicol Lett 2013; 218(1): 2-9.

Mai TC, Delanaud S, Bach V, Braun A, Pelletier A, de Seze R. Effect of non-thermal radiofrequency on body temperature in mice. Sci Rep 2020;10(1): 5724.

Maskey D, Kim M, Aryal B, Pradhan J, Choi IY, Park KS, Son T, Hong SY, Kim SB, Kim HG, Kim MJ. Effect of 835 MHz radiofrequency radiation exposure on calcium binding proteins in the hippocampus of the mouse brain. Brain Res 2010; 1313:232-41.

McNamee JP, Chauhan V. Radiofrequency radiation and gene/protein expression: A review. Radiat Res 2009; 172(3):265-87.

Megha K, Deshmukh PS, Banerjee BD, Tripathi AK, Ahmed R, Abegaonkar MP. Low intensity microwave radiation induced oxidative stress, inflammatory response and DNA damage in rat brain. Neurotoxicology 2015; 51:158-65.

Panagopoulos DJ, Karabarbounis A, Margaritis LH. Mechanism for action of electromagnetic fields on cells. Biochem Biophys Res Commun 2002; 298(1):95-102.

Panagopoulos DJ, Messini N, Karabarbounis A, Philippetis AL, Margaritis LH. A mechanism for action of oscillating electric fields on cells. Biochem Biophys Res Commun 2000; 272(3):634-40.

Repacholi MH. Health risks from the use of mobile phones. Toxicol Lett. 2001; 120(1-3):323-31.

Repacholi MH. Low-level exposure to radiofrequency electromagnetic fields: health effects and research needs. Bioelectromagnetics 1998; 19(1):1-19.

Rérole AL, Jego G, Garrido C. Hsp70: Anti-apoptotic and tumorigenic protein. Methods Mol Biol 2011; 787: 205-30.

Singh R, Nath R, Mathur AK, Sharma RS. Effect of radiofrequency radiation on reproductive health. Indian J Med Res 2018; 148(Suppl): S92-S99.

Sommer AM, Streckert J, Bitz AK, Hansen VW, Lerchl A. No effects of GSM-modulated 900 MHz electromagnetic fields on survival rate and spontaneous development of lymphoma in female AKR/J mice. BMC Cancer 2004; 4: 77.

Stuchly MA. Interaction of radiofrequency and microwave radiation with living systems: A review of mechanisms. Radiat Environ Biophys 1979; 16(1):1-14.

Trošić I, Pavičić I, Marjanović AM, Bušljeta I. Non-thermal biomarkers of exposure to radiofrequency/microwave radiation. Arh Hig Rada Toksikol 2012; 63 Suppl 1:67-73.

Trosić I, Pavicić I, Milković-Kraus S, Mladinić M, Zeljezić D. Effect of electromagnetic radiofrequency radiation on the rats' brain, liver and kidney cells measured by comet assay. Coll Antropol 2011; 35(4):1259-64.

Vijayalaxmi, Scarfi MR. International and national expert group evaluations: Biological/health effects of radiofrequency fields. Int J Environ Res Public Health 2014; 11(9):9376-408.

Vornoli A, Falcioni L, Mandrioli D, Bua L, Belpoggi F. The contribution of in vivo mammalian studies to the knowledge of adverse effects of radiofrequency radiation on human health. Int J Environ Res Public Health 2019; 16(18):3379.

Wyde ME, Horn TL, Capstick MH, Ladbury JM, Koepke G, Wilson PF, Kissling GE, Stout MD, Kuster N, Melnick RL, Gauger J, Bucher JR, McCormick DL. Effect of cell phone radiofrequency radiation on body temperature in rodents: Pilot studies of the National Toxicology Program's reverberation chamber exposure system. Bioelectromagnetics 2018; 39(3):190-199.

Xing F, Zhan Q, He Y, Cui J, He S, Wang G. 1800MHz microwave induces p53 and p53-mediated caspase-3 activation leading to cell apoptosis in vitro. PLoS One 2016; 11(9):e0163935.

Yakymenko I, Tsybulin O, Sidorik E, Henshel D, Kyrylenko O, Kyrylenko S. Oxidative mechanisms of biological activity of low-intensity radiofrequency radiation. Electromagn Biol Med 2016; 35(2):186-202.

Yokus B, Akdag MZ, Dasdag S, Cakir DU, Kizil M. Extremely low frequency magnetic fields cause oxidative DNA damage in rats. Int J Radiat Biol 2008; 84(10):789-95.

Zhang JP, Zhang KY, Guo L, Chen QL, Gao P, Wang T, Li J, Guo GZ, Ding GR. Effects of 1.8 GHz radiofrequency fields on the emotional behavior and spatial memory of adolescent mice. Int J Environ Res Public Health 2017; 14(11):1344.

Zmyślony M, Politanski P, Rajkowska E, Szymczak W, Jajte J. Acute exposure to 930 MHz CW electromagnetic radiation in vitro affects reactive oxygen species level in rat lymphocytes treated by iron ions. Bioelectromagnetics 2004; 25(5):324-8.

SUPPLEMENTARY INFORMATION

Supplementary Table 1: Primer sequences

Gene name	Sequence (5'-3')
P53 forward	GAGGCCGGCTCTGAGTAT
P53 reverse	CGGATCTTGAGGGTGAAAT
HSP 70 forward	GCTGACCAAGATGAAGGAGAT
HSP 70 reverse	GCTGCGAGTCGTTGAAGTAG
Beta-actin forward	TCAAGATCATTGCTCCTCCT
Beta-actin reverse	GTTTGCTCCAACCAACTGC